Chemical Science

ROYAL SOCIETY OF CHEMISTRY

EDGE ARTICLE

View Article Online
View Journal | View Issue

Check for updates

Cite this: *Chem. Sci.*, 2020, **11**, 839

All publication charges for this article have been paid for by the Royal Society of Chemistry

Received 6th November 2019
Accepted 27th November 2019

DOI: 10.1039/c9sc05601g

rsc.li/chemical-science

Visible-light-driven spirocyclization of epoxides *via* dual titanocene and photoredox catalysis†

Shuangjie Lin,‡ Yuqing Chen,‡ Fusheng Li, Caizhe Shi and Lei Shi *

We describe the synergistic utilization of titanocene/photoredox dual catalysis driven by visible light for the radical opening/spirocyclization of easily accessible epoxyalkynes. This environmentally benign process uses the organic donor–acceptor fluorophore 2,4,5,6-tetra(9*H*-carbazol-9-yl)isophthalonitrile (4CzIPN) as a photocatalyst and Hantzsch ester (HE) as an electron donor instead of stoichiometric metallic reductants. The photocatalytic conditions showed exceptionally high reactivity for the synthesis of privileged and synthetically challenging spirocycles featuring a spiro all-carbon quaternary stereocenter. Cyclic voltammetry (CV) studies suggest that $Cp_2Ti^{III}Cl$ is the catalytically active species.

Over the last few decades, radical-based transformations have been increasingly used in organic synthesis due to their salient features, such as ease of generation, mild reaction conditions, and broad functional group compatibility.[1,2] As a mild single-electron-transfer (SET) reagent, titanocene monochloride ($Cp_2Ti^{III}Cl$) is considered a formidable tool in contemporary radical chemistry due to its ability to promote various fundamental radical-based transformations.[3–7] $Cp_2Ti^{III}Cl$ was first introduced by Nugent and RajanBabu as a very mild stoichiometric reagent for the reductive opening of epoxides.[8–11] Later, the catalytic conditions developed by Gansäuer *et al.* (Scheme 1a)[12] employing stoichiometric amounts of active metals in combination with 2,4,6-collidine·HCl further expanded its applications and led to the discovery of a number of novel transformations.[13–16] The key to success was the formation of a stable complex **A** in reactions while decreasing the concentration of active $Cp_2Ti^{III}Cl$.[17,18] We were interested in the radical opening/cyclization reaction of epoxides which has attracted considerable attention from the synthetic community and has been used numerous times in the synthesis of natural products.[19,20] Nevertheless, this reaction required stoichiometric metallic reductants and proceeded slowly particularly with sterically hindered substrates even with high catalyst loading.[21] Therefore, the development of an eco-friendly and efficient catalytic system with an expanded substrate scope is highly desirable.

In recent years metallaphotoredox catalysis has been a new and rapidly growing research subject.[22–29] Photoredox processes can directly modulate the oxidation state of metals by electron transfer (ET).[30–33] Given that the generation of Ti^{III} is a SET process, we envisioned that the reduction could be facilitated by a photoredox-controlled process while overcoming the aforementioned limitations. On the other hand, spirocycles bearing a chiral spiro all-carbon quaternary carbon are particularly attractive synthetic targets in pharmaceutical development (Scheme 1c).[34–36] Such privileged rigid 3D structures offer the concomitant ability to project functionalities in all three-dimensional orientations and led to enhanced pharmacological activities of molecules. Thus significant attention has been

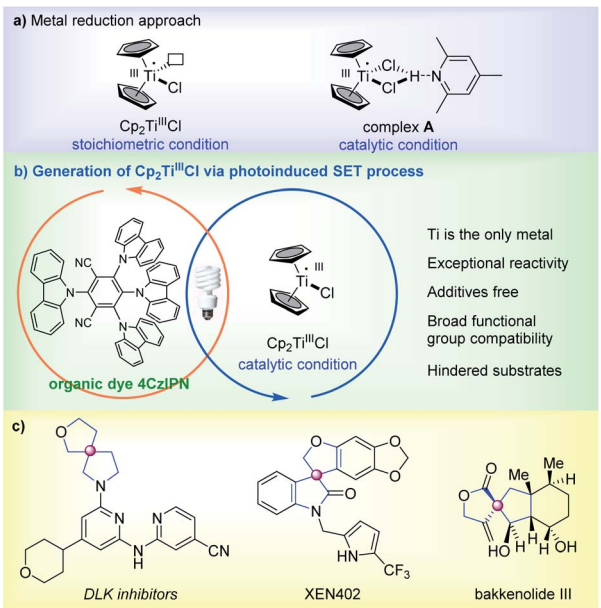

Scheme 1 $Cp_2Ti^{III}Cl$ mediated radical opening/spirocyclization of epoxides; (a) generation of Ti^{III} *via* a metal reduction approach; (b) dual titanocene/photoredox catalysis; (c) examples of drugs and natural products containing heterospirocycles.

Zhang Dayu School of Chemistry, State Key Laboratory of Fine Chemicals, Dalian University of Technology, Dalian, 116024, China. E-mail: shilei17@dlut.edu.cn

† Electronic supplementary information (ESI) available. See DOI: 10.1039/c9sc05601g

‡ These authors contributed equally.

Table 1 Optimization of the reaction conditions

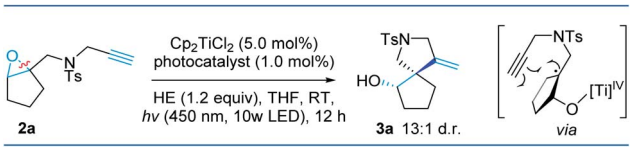

Entry	Conditions[a]	Yield (%)[b]
1	$[Ir(dtbbpy)(ppy)_2]PF_6$ **1a**	96
2	23 W CFL instead of 450 nm LED, **1a**, 16 h	95
3	2 mol% Ti, **1a**, 24 h	94
4	4CzIPN **1b**, 16 h	94
5	No titanocene	0
6	No HE	0
7	No photocatalyst	0
8	No *hv*	0
9	DCE instead of THF, **1a**	93
10	Et_3N instead of HE, **1a**	9
11	Na_2CO_3 (1.0 equiv.) as additive, **1a**	0

[a] Reaction conditions: **2a** (100 mg, 0.1 M in THF). [b] Isolated yield.

paid to their synthesis.[37,38] Against this backdrop, here we describe our efforts on the synthesis of various heterospirocycles with the aid of photoredox catalysis.

We chose epoxyalkyne **2a** as a model substrate for optimization of reaction conditions. After a systematic variation of different reaction parameters, we were pleased to identify the optimal reaction conditions in which a mixture of Cp_2TiCl_2 (5.0 mol%), $[Ir(dtbbpy)(ppy)_2]PF_6$ (**1a**, 1.0 mol%, $E_{1/2}^{III/II} = -1.51$ V *vs.* SCE in MeCN), HE (1.2 equiv.) and **2a** (1.0 equiv.) in THF at room temperature under the irradiation of a 10 W 450 nm light emitting diode (LED) lamp for 12 hours afforded the desired product **3a** in an excellent yield of 96% (13 : 1 d.r.) upon isolation (entry 1). Using a commercial 23 W compact fluorescent lamp (CFL) instead of the 10 W 450 nm LED did not compromise the overall yield of the reaction (entry 2). Notably, when the loading of Cp_2TiCl_2 was decreased to as low as only 2.0 mol%, the reaction still led to full conversion and produced **3a** in 95% yield (entry 3). Further screening of other photosensitizers revealed that the cheap and readily obtained organic dye 4CzIPN **1b** is a competent alternative, which led to full conversion with 94% isolated yield (entry 4). Importantly, the reaction did not proceed in the absence of Cp_2TiCl_2, HE, the photocatalyst, or visible light (entries 5–8). Various solvents, including DMF, MeOH, DMSO, and MeCN, were screened, and they all resulted in poor conversion. The use of other organic electron donors, such as triethylamine, triethanolamine, and ascorbic acid, afforded the product in poor yield.

With satisfactory reaction conditions established, we then explored the scope of the cyclization reaction using 4CzIPN as the photosensitizer. Positively, the cyclization reaction worked well and afforded the desired variably heterospirocyclic products in good to excellent yield (Tables 2 and 3). The reaction allows the rapid construction of various 5/5, 5/6, 5/7 and 5/8 spiro-ring fused systems (**3a–3k**) bearing tetrahydrofuran or

Table 2 Scope of 5-*exo* and 6-*exo* cyclization[a,b,c,d]

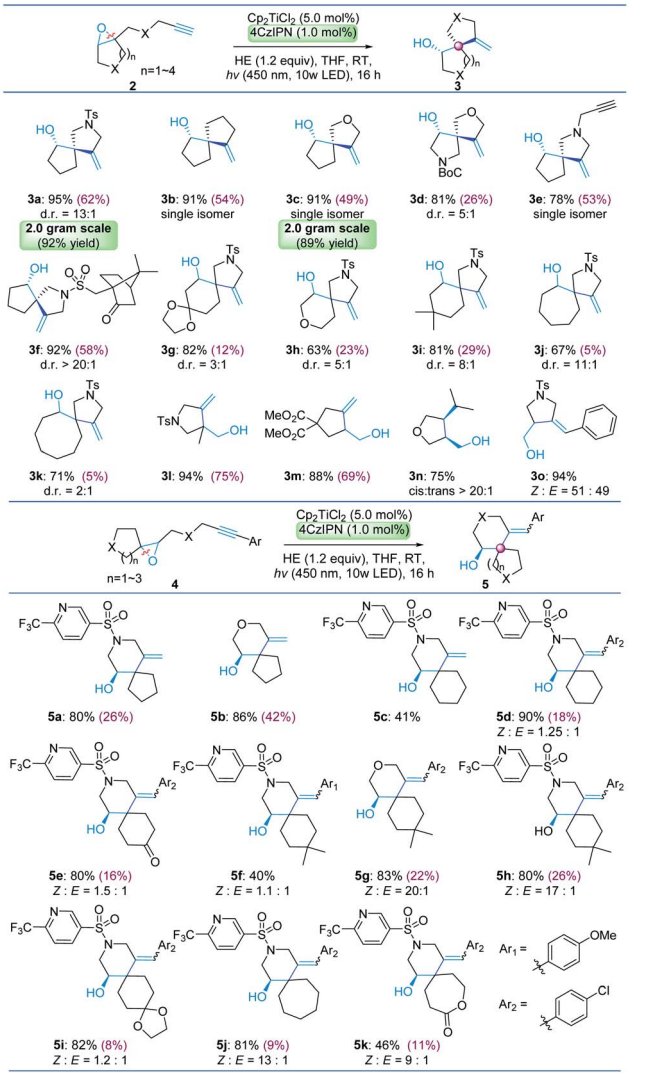

[a] Reaction conditions: **2** and **4** (100 mg, 0.1 M in THF). [b] Isolated yield. [c] **3c**, **3e** and **3f** were synthesized from enantiomer pure epoxides. [d] Yields within parentheses are based on catalytic conditions using metal as a reductant: $CpTi_2Cl_2$ (5 mol%), Zn (2.0 eq.), coll·HCl (2.5 eq.), THF, 20 hours.

pyrrolidine motifs *via* the 5-*exo* cyclization pathway. Interesting, the diastereoselectivity of the cyclization reaction is highly correlated with the ring size in the substrates. Heterospirocycles containing a 5/5 spiro-ring fused system (**3a–3f**) were obtained with surprisingly high diastereoselectivity. In some cases (**3b**, **3c**, and **3e**) only a single isomer was obtained. The product **3d** with a sterically hindered *t*-butyloxy carbonyl (Boc) protecting group on the N atom was obtained with reduced diastereoselectivity (5 : 1 d.r.). The diastereoselectivities dropped in 5/6, 5/7 and 5/8 spiro-ring fused systems. Given that enantioenriched epoxides could be easily obtained (*e.g. via* sharpless asymmetric epoxidation), this strategy provides access to optically active spirocycles featuring an all-carbon quaternary stereocenter with the transfer of stereochemical information from

Table 3 Additive effect on Ti-catalyzed cyclization[a,b]

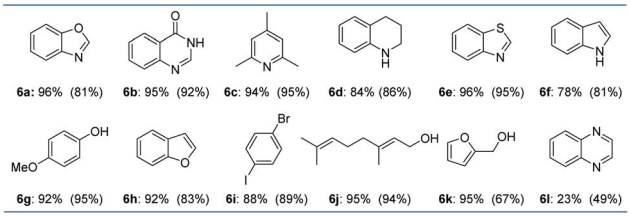

[a] In all cases, **2l** was used as the substrate and the yield of **3l** was determined with ^{1}H NMR. [b] Values within parentheses are recovery yields of the additives determined with ^{1}H NMR.

epoxides (**3c**, **3e** and **3f**). Bis-heterospirocyclic scaffolds were frequently employed in pharmaceutical chemistry. For example, bis-heterospirocyclic **3d** is the core structure of DLK inhibitors[39] and XEN402 (ref. 40) (scheme 1c), which are used for treating neurodegeneration and congenital erythromelalgia respectively. Furthermore, 6-*exo* cyclization was also investigated under the standard conditions and smoothly produced a serious of drug-like 6-(trifluoromethyl)-3-pyridinesulfonyl piperidine derivatives including 6/5, 6/6 and 6/7 spiro-ring fused systems (**5a–5k**) in generally excellent yields. Moreover, cyclization reactions with epoxy-alkynes afforded products containing exocyclic-alkenes and free alcohols which were suitable for further functionalization. This approach provides access to a broad range of novel spirocyclic piperidine and pyrrolidine spirocycles which could be of interest to synthetic and medicinal chemists.

To examine the scalability of the reaction, gram-scale synthesis of **3a** and **3c** was performed under the standard conditions with 23 W CFL irradiation. Pleasingly, 92% (**3a**) and 89% (**3c**) isolated yields were obtained respectively without any deterioration. Furthermore, an additive-based investigation[41] was performed and the results are summarized (Table 3). From this screening, we found that 11 out of 12 additives have no adverse impact on the yield of the reaction. The additives were recovered after the reaction, including benzoxazole **6a**, quinazolinone **6b**, collidine **6c**, tetrahydroquinoline **6d**, benzothiazole **6e**, indole **6f**, and benzofuran **6h**. However, quinoxaline **6l** strongly inhibited Ti catalysis and **3l** was produced in only 23% yield. Notably, the reaction is compatible with various functional groups including phenols **6g**, free alcohols and alkene **6j**, iodobenzene **6i**, ester **3m**, ether **3n**, dioxolane **5i**, lactone **5k**, and alkyne **3e**. The generality of the dual Ti/4CzIPN catalysis system was further demonstrated by a highly related hydrogen transfer reaction of epoxides which could exclusively provide anti-Markovnikov alcohols (see the ESI S8†). The low-cost of 4CzIPN, broad compatibility with sensitive functional groups, and simple operation conditions are appealing for laboratory and industrial applications.

Importantly, the reactions were re-subjected to metal reduction catalytic conditions for comparison with the photocatalytic conditions and the yields are shown within parentheses (Table 2[d]). It clearly showed that the yields were generally lower. Particularly, we found that the yields dropped dramatically as the steric encumbrance of the substrates increased. For example, substrates containing dioxolane (**2g**, **4i**) or a 7/8-membered-ring (**2j**, **2k**, **4j**) afforded the products (**3g**, **5i**, **3j**, **3k**, **5j**) in less than 10% yield with the recovery of the starting materials.

Catalytic species and mechanistic studies

To further understand the exceptional reactivity of the photocatalytic reaction system and the mechanism, a series of experiments were performed. First, the mixture of Cp_2TiCl_2, the photocatalyst (**1a** or **1b**) and HE in THF was irradiated under a 23 W CFL or a 450 nm LED at room temperature. The color change from red (Cp_2TiCl_2) to green indicates that a Ti^{III} species was formed (Fig. 1b). The results of analysis by ultraviolet-visible (UV-vis) spectroscopy further revealed that the reduction is fast. It was nearly complete within 20 minutes (Fig. 1a). On the other hand, no change of color was observed in the dark even at elevated temperatures, indicating that ground-state SET was not operative. The initial electron transfer during the SET process was investigated by fluorescence quenching experiments (Fig. 1c). The luminescence of **1a** at its λ_{max} (591 nm) in degassed THF was readily quenched by Cp_2TiCl_2, exhibiting Stern–Volmer kinetics with a rate of 3.8×10^9 L M^{-1} S^{-1}. HE also quenched the luminescence of **1a** with a rate of 4.5×10^7 L M^{-1} S^{-1}. Therefore, both oxidative and reductive quenching of the excited state of **1a** can occur.

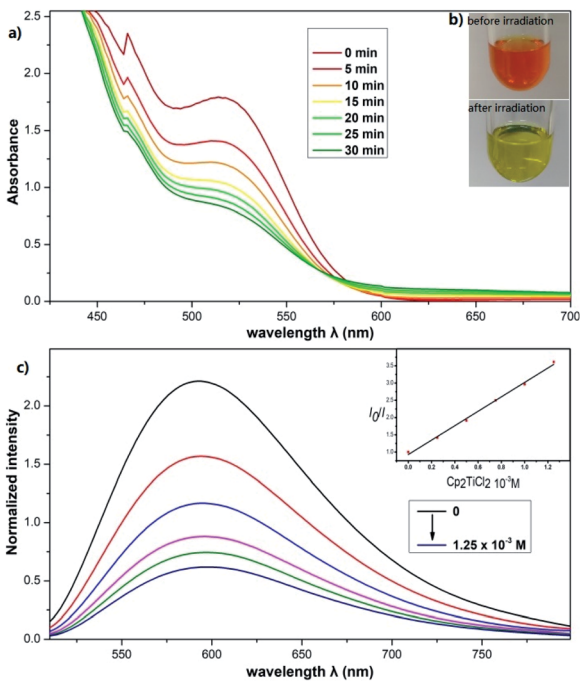

Fig. 1 (a) UV-vis spectra showing the reduction of Cp_2TiCl_2 upon photoirradiation of a solution of Cp_2TiCl_2, $[Ir(dtbbpy)(ppy)_2]PF_6$ and HE in THF; the peak at 515 nm corresponds to Cp_2TiCl_2. (b) Photo-irradiation (23 W CFL) of the mixture for 30 min. (c) $[Ir(dtbbpy)(ppy)_2]PF_6$ emission quenching by Cp_2TiCl_2. Experimental details are found in the ESI, S2.†

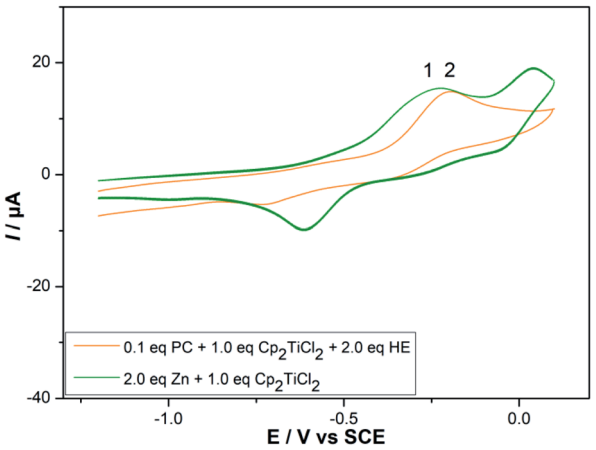

Fig. 2 Cyclic voltammetry of 2 mM Cp_2TiCl_2/Zn (green line) and 2 mM Cp_2TiCl_2/[Ir(dtbbpy)(ppy)$_2$]PF_6/HE (orange line) recorded on a glassy carbon disk electrode with $\nu = 0.1$ V s^{-1} in 0.2 M Bu_4NPF_6/THF. Experimental details are found in the ESI, S4.† The values are given in V *vs.* SCE and can be converted to V *vs.* Fc^+/Fc by subtracting 0.52 V.

Cyclic voltammetry (CV) studies were carried out and the results are shown in Fig. 2. In line with the previous CV studies of Zn/Cp_2TiCl_2 solutions in THF (green line), the broad oxidation wave appearing at −0.26 V (*vs.* SCE) is assigned to the $(Cp_2Ti^{III}Cl)_2$ dimer and $Cp_2Ti^{III}Cl$ monomer couple (designated **1/2**).[17,42] Interestingly, CV studies of Ti^{III} species generated under photoreductive conditions (orange line) revealed the main oxidation wave appearing at −0.22 V (*vs.* SCE) which corresponds to the $Cp_2Ti^{III}Cl$ monomer. One concern was the intrinsic instability of Cp_2TiCl_2 under visible light which would decompose by losing a cyclopentadienyl ligand.[43] Nevertheless, in the preliminary studies we found that the $Cp_2Ti^{III}Cl$ species exhibits special stability under photoreductive conditions (for detailed Experiments and discussion, please see the ESI S9†). Furthermore, the CV analysis of Zn/$CpTiCl_3$ showed the main oxidation wave appearing at −0.63 V (*vs.* SCE) (see the ESI S4†). Therefore, the possibility of generation of the $CpTi^{III}Cl_2$ species *via* losing a cyclopentadienyl ligand under light could be ruled out.

Additionally, the reaction profiles were examined and are shown in Fig. 3. The photocatalytic reaction did not show an obvious incubation period. Moreover, the reactions proceeded pretty fast and completed (full conversion of substrates) within around 2 hours with **2a** (red solid line) and even more sterically hindered **4i** (blue solid line). In contrast, under the metal reduction catalytic conditions, the reactions proceeded slowly for the same substrates **2a** (red dashed line) and **4i** (blue dashed line). These results clearly showed the advantage of the current photocatalytic system. Kinetically, complex **A** (Scheme 1a) formed under metal reduction conditions is less reactive presumably due to the fact that it has no free coordination sites. In contrast, $Cp_2Ti^{III}Cl$ generated under photocatalytic conditions has a vacant site allowing the oxygen atom of the epoxide to perform a SET through an inner-sphere mechanism efficiently. Furthermore, the *in situ*-generated HP cation **7**, which has a low p*K*a value compared with the collidine cation, can enhance the rate of protonation of the Ti^{IV}-alkoxy bond in the catalytic cycle. This is supported by the fact that the reaction is significantly inhibited by the addition of Na_2CO_3 or using triethylamine as a reductant (Table 1, entry 10 and 11).

Based on these results, we tentatively propose the following catalytic cycle in Fig. 5. First, Cp_2TiCl_2 is reduced to $Cp_2Ti^{III}Cl$ by a photocatalyst (such as excited Ir^{III}). The strong oxidant Ir^{IV} species is then reduced by HE to Ir^{III} and produces $HE^{+\bullet}$ concurrently. $Cp_2Ti^{III}Cl$ promoted the reductive opening of the epoxides. The resulting carbon radical **8** intramolecularly adds

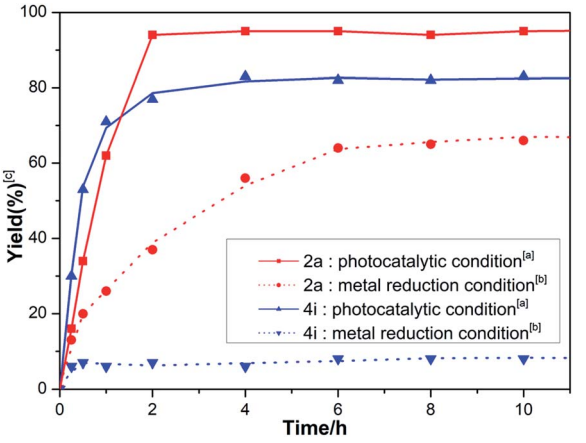

Fig. 3 Reaction profiles for **2a** and **4i** (200 mg, 0.1 M in THF). [a] Photocatalytic conditions: 450 nm 10 W LED, **1a** (1 mol%), Cp_2TiCl_2 (5 mol%), HE (1.2 eq). [b] Metal reduction conditions: $CpTi_2Cl_2$ (5 mol%), Zn (2.0 eq.), coll·HCl (2.5 eq.). [c] The yields of **3a** or **5i** were determined with ^{1}H NMR.

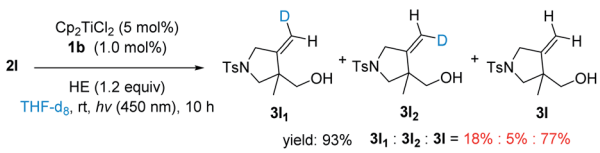

Fig. 4 Cyclization of **2l** in the presence of THF-d_8.

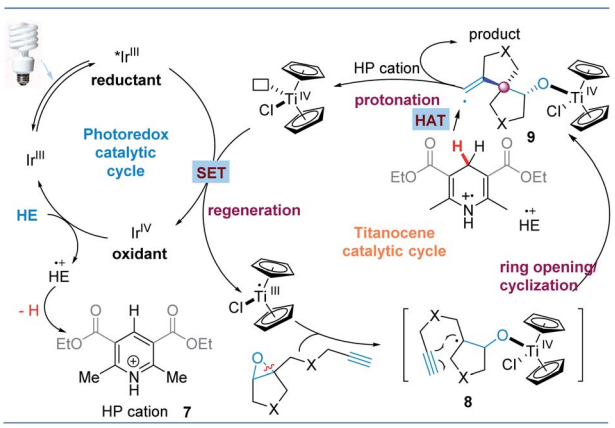

Fig. 5 Proposed catalytic mechanism.

to the pendant alkyne to construct the spirocyclic structure. The newly formed vinyl radical **9** can abstract a C4–H hydrogen atom of the HE radical cation ($HE^{+\bullet}$). This is because $HE^{+\bullet}$ has a low homolytic bond-dissociation free energy for the C4–H bond (this energy requirement is 31.4 kcal mol^{-1} for acetonitrile).[44] Deuterium labeling experiments also shows that THF may offer a H source for hydrogen atom transfer (Fig. 4). The *in situ*-produced Ti–oxygen bond is protonated by the HP cation and Ti^{IV} is released as well as the cyclization product. Finally, Ir^{III} can regenerate $Cp_2Ti^{III}Cl$ for the next catalytic cycle.

Conclusions

In summary, we report a novel and greener dual catalyst system consisting of titanocene and the organic dye 4CzIPN for the radical spirocyclization of epoxides under photocatalytic conditions. This operationally simple, scalable, and efficient method provides a strategically distinct manner for the assembly of heterospirocycles featuring a spiro all-carbon quaternary stereocenter. Unlike the metal reduction catalytic conditions, mechanistic studies suggest that under photocatalytic conditions, Ti^{III} is present as Cp_2TiCl which is readily accessible to epoxides. As expected, the photocatalytic conditions showed exceptional high reactivity for the assembly of heterospirocycles. In this respect, the photocatalytic approach complements the metal reduction approach. Development of new transformations based on photocatalytic reactions is currently under way in our laboratory.

Conflicts of interest

There are no conflicts to declare.

Acknowledgements

We are grateful to the Fundamental Research Funds for the Central Universities (No. DUT19LK31). We thank WATTCAS CHEM-TECH Co., Ltd. for kindly providing the photoreactor.

Notes and references

1 M. P. Plesniak, H. Huang and D. J. Procter, *Nat. Rev. Chem.*, 2017, **1**(10), 77.
2 A. Studer, *Encyclopedia of Radicals in Chemistry, Biology and Materials*, John Wiley & Sons, Ltd., 2012.
3 A. Rosales, I. Rodríguez-García, J. Muñoz-Bascón, E. Roldan-Molina, N. M. Padial, L. P. Morales, M. García-Ocaña and J. E. Oltra, *Eur. J. Org. Chem.*, 2015, **21**, 4567–4591.
4 Y. Zhang, E. Vogelsang, Z. Qu, S. Grimme and A. Gansäuer, *Angew. Chem., Int. Ed.*, 2017, **56**(41), 12654–12657.
5 K. Ye, T. MCallum and S. Lin, *J. Am. Chem. Soc.*, 2019, **141**(24), 9548–9554.
6 L. H. Leijendekker, J. Weweler, T. M. Leuther and J. Streuff, *Angew. Chem., Int. Ed.*, 2017, **56**(22), 6103–6106.
7 J. Muñoz-Bascón, I. Sancho-Sanz, E. Álvarez-Manzaneda, A. Rosales and J. E. Oltra, *Chem.–Eur. J.*, 2012, **18**(45), 14479–14486.
8 W. A. Nugent and T. V. RajanBabu, *J. Am. Chem. Soc.*, 1988, **110**, 8561–8562.
9 T. V. RajanBabu and W. A. Nugent, *J. Am. Chem. Soc.*, 1994, **116**(3), 986–997.
10 M. L. H. Green and C. R. Lucas, *J. Chem. Soc., Dalton Trans.*, 1972, 1000–1003.
11 J. M. Birmingham, A. K. Fischer and G. Wilkinson, *Naturwissenschaften*, 1955, **42**, 96.
12 A. Gansäuer, H. Bluhm and M. Pierobon, *J. Am. Chem. Soc.*, 1998, **120**(49), 12849–12859.
13 J. Justicia, J. L. Oller-López, A. G. Campaña, J. E. Oltra, J. M. Cuerva, E. Buñuel and D. J. Cárdenas, *J. Am. Chem. Soc.*, 2005, **127**(42), 14911–14921.
14 J. Friedrich, M. Dolg, A. Gansäuer, D. Geich-Gimbel and T. Lauterbach, *J. Am. Chem. Soc.*, 2005, **127**(19), 7071.
15 J. Friedrich, K. Walczak, M. Dolg, F. Piestert, T. Lauterbach, D. Worgull and A. Gansäuer, *J. Am. Chem. Soc.*, 2008, **130**(5), 1788–1796.
16 A. Gansäuer, D. Worgull, K. Knebel, I. Huth and G. Schnakenburg, *Angew. Chem., Int. Ed.*, 2009, **48**(47), 8882–8885.
17 A. Gansäuer, C. Kube, K. Daasbjerg, R. Sure, S. Grimme, G. D. Fianu, D. V. Sadasivam and R. A. Flowers, *J. Am. Chem. Soc.*, 2014, **136**(4), 1663–1671.
18 J. Gordon, S. Hildebrandt, K. R. Dewese, S. Klare, A. Gansäuer, T. V. RajanBabu and W. A. Nugent, *Organometallics*, 2018, **37**(24), 4801–4809.
19 N. M. Padial, E. Roldan-Molina, A. Rosales, M. Álvarez-Corral, I. Rodríguez-García, M. Muñoz-Dorado and J. E. Oltra, *Studies in Natural Products Chemistry*, 2018, vol. 55, pp. 31–71.
20 S. P. Morcillo, D. Miguel, A. G. Campana, L. Alvarez De Cienfuegos, J. Justicia and J. M. Cuerva, *Org. Chem. Front.*, 2014, **45**(25), 15–33.
21 L. Shi, K. Meyer and M. F. Greaney, *Angew. Chem., Int. Ed.*, 2010, **49**(48), 9250–9253.
22 J. Twilton, C. C. Le, P. Zhang, M. H. Shaw, R. W. Evans and D. W. C. MacMillan, *Nat. Rev. Chem.*, 2017, **1**(7), 52.
23 C. K. Prier, D. A. Rankic and D. W. C. MacMillan, *Chem. Rev.*, 2013, **113**(7), 5322–5363.
24 B. L. Tóth, O. Tischler and Z. Novák, *Tetrahedron Lett.*, 2016, **57**(41), 4505–4513.
25 I. Ghosh, L. Marzo, A. Das, R. Shaikh and B. König, *Acc. Chem. Res.*, 2016, **49**(8), 1566–1577.
26 J. C. Tellis, C. B. Kelly, D. N. Primer, M. Jouffroy, N. R. Patel and G. A. Molander, *Acc. Chem. Res.*, 2016, **49**(7), 1429–1439.
27 D. Staveness, I. Bosque and C. R. J. Stephenson, *Acc. Chem. Res.*, 2016, **49**(10), 2295–2306.
28 K. L. Skubi, T. R. Blum and T. P. Yoon, *Chem. Rev.*, 2016, **116**(17), 10035–10074.
29 J. A. Milligan, J. P. Phelan, S. O. Badir and G. A. Molander, *Angew. Chem.*, 2019, **131**(19), 6212–6224.
30 K. Shimomaki, K. Murata, R. Martin and N. Iwasawa, *J. Am. Chem. Soc.*, 2017, **139**(28), 9467–9470.
31 Q. Meng, S. Wang and B. König, *Angew. Chem., Int. Ed.*, 2017, **56**(43), 13426–13430.

32 Z. Zhang, R. B. Richrath and A. Gansäuer, *ACS Catal.*, 2019, **9**(4), 3208–3212.
33 D. C. Fabry and M. Rueping, Merging Visible Light, *Acc. Chem. Res.*, 2016, **49**(9), 1969–1979.
34 Y. Zheng and C. M. Tice, *Expert Opin. Drug Discovery*, 2016, **11**(9), 831–834.
35 Y. Zheng, C. M. Tice and S. B. Singh, *Bioorg. Med. Chem. Lett.*, 2014, **24**(16), 3673–3682.
36 L. K. Smith and I. R. Baxendale, *Org. Biomol. Chem.*, 2015, **13**(39), 9907–9933.
37 N. J. Flodén, A. Trowbridge, D. Willcox, S. M. Walton, Y. Kim and M. J. Gaunt, *J. Am. Chem. Soc.*, 2019, **141**(21), 8426–8430.
38 N. A. Weires, Y. Slutskyy and L. E. Overman, *Angew. Chem., Int. Ed.*, 2019, **58**(25), 8561–8565.
39 B. A. Chalyk, M. V. Butko, O. O. Yanshyna, K. S. Gavrilenko, T. V. Druzhenko and P. K. Mykhailiuk, *Chem.–Eur. J.*, 2017, **23**(66), 16782–16786.
40 S. K. Bagal, A. D. Brown, P. J. Cox, K. Omoto, R. M. Owen, D. C. Pryde, B. Sidders, S. E. Skerratt, E. B. Stevens, R. I. Storer and N. A. Swain, *J. Med. Chem.*, 2013, **56**(3), 593–624.
41 K. D. Collins and F. Glorius, *Nat. Chem.*, 2013, **5**(7), 597–601.
42 R. J. Enemærke, J. Larsen, T. Skrydstrup and K. Daasbjerg, *J. Am. Chem. Soc.*, 2004, **126**(25), 7853–7864.
43 M. Tehfe, J. Lalevée, F. Morlet-Savary, B. Graff and J. Fouassier, *Macromolecules*, 2011, **45**(1), 356–361.
44 X. Zhu, H. Li, Q. Li, T. Ai, J. Lu, Y. Yang and J. Cheng, *Chem.–Eur. J.*, 2003, **9**(4), 871–880.